Mesoscale Convective Complexes (or Systems)

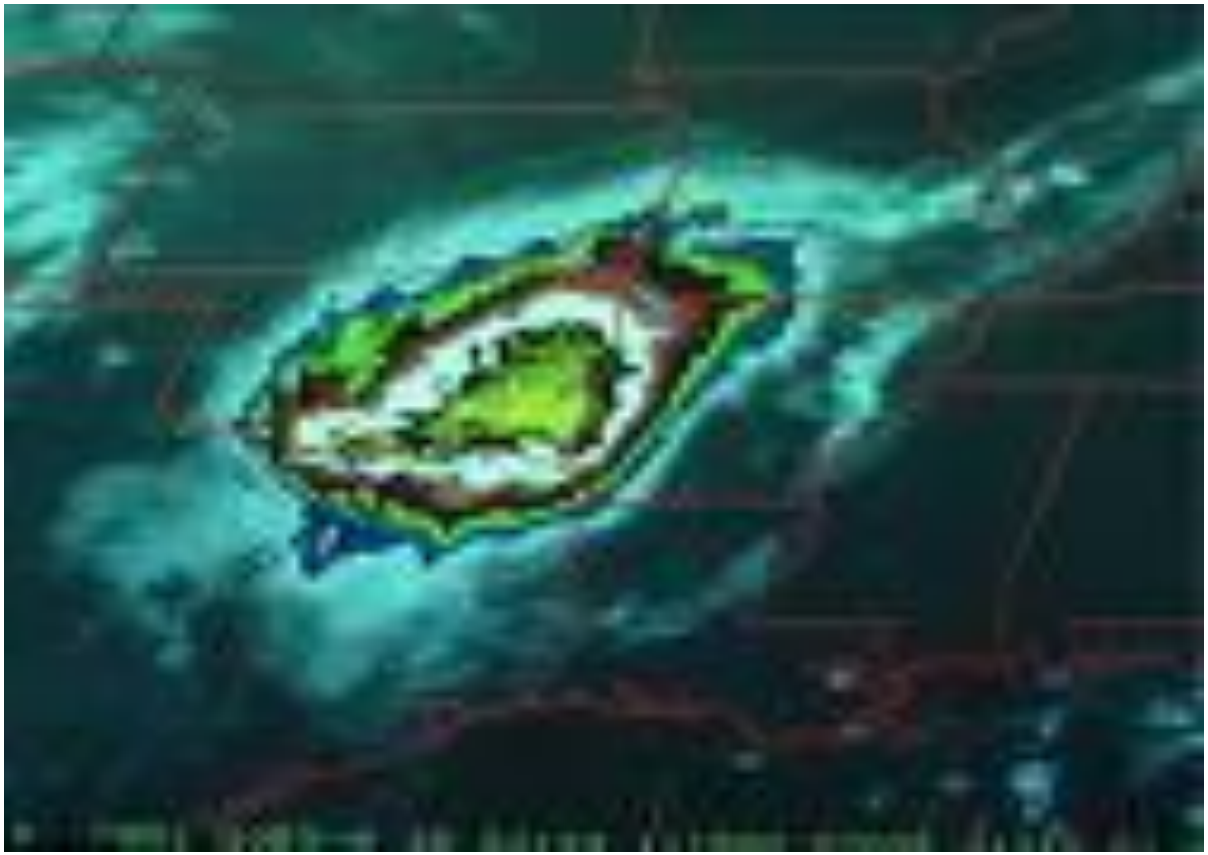

What is an MCC

- Mesoscale Convectiv Complexes (MCCs) are organized clusters of storms that have to meet some size and shape criteria:

* -32C IR temp > 100,000 km^2

* -52C IR temp > 50,000 km^2

* eccentricity > 0.7 (means it has to be rather round)

Cotton et al. “A composite model of Mesoscale Convective Complexes”

- Methodology

* composite analysis: compositing emphasizes features in common; noise gets averaged out but small-scale “real” features also get averaged out

* 134 cases, stratified according to MCC life cycle:

Life cycle stages

- Pre-MCC: 3 hr before initial stage
- Initial: -52C cloud shield > 50,000 km2
- Growth: midpoint between initial & mature
- Mature: maximum -52C cloud shield
- Decay: midpoint between mature & decay
- Dissipation: -52C cloud shield < 50,000 km2
- Post-MCC: 3 hr after dissipation

- Cotton et al also looked at the period 12 hrs before initiation
- Focus was on well-organized MCCs without other MCC/MCSs in vicinity. Cases not meeting these criteria were put in a “marginal” class
- Analyzed 00 and 12 UTC radiosonde data to a grid centered on the MCC. Data were interpolated on isentropic sfcs using Barnes OA scheme. 2x2 latitude grid; isentropic spacing = 3K (≈500-1000 m) from sfc up to 360K and 10K from 360K up. Assuming sfc θ=290K in spring/summer, 360K ≈ (360-290K)/3.3K/km ≈ 15 km

Two approaches to compositing

- Composite before analysis
- Analysis before composite

Evolution of MCC environment

- Pre-MCC (12 hr before)/Initial stage

*prominent features include:

** strong southerly low-level jet. Recall the LLJ is likely related to 3 processes (inertial oscillation of ageostrophic wind, thermal wind adjustment to diurnal PBL heating over sloped terrain, adjustment to synoptically-induced pressure changes like lee side troughing)

** The LLJ promotes the MCC development in 3 main ways

1) Moisture advection – to enhance the convective instability
2) differential temperature advection – low-level warm advection destabilizes the temperature profile
3) Lifting is produced by frontal overrunning and/or convergence at the “nose” of the LLJ. Notice on Cotton et al. Fig 6 the nose of the LLJ coincides almost exactly with the location of initial-stage MCCs

**The initial MCC is at the nose of a “ridge” in the low-level θe. The θe ridge is fairly well aligned with the LLJ, again emphasizing the role of the LLJ in advecting warm, moist air into the MCC

** The initial location of the composite MCC is located almost exactly coincident with the maximum 700-400 mb mixing ratio, indicating that mid-level moisture is supportive of MCC development. This is in contrast to common view that mid-level dryness promotes severe storms.

The midlevel moistening is due to:

1) convection preceding MCC, acting to transport boundary-layer moisture upward

2) a SW monsoon flow that develops in late summer over the SW USA due to the strong elevated heat source in the desert region between the Rockies and the Pacific.

*Initial MCC is also located almost exactly at the max in warm advection at 700 mb.

The warm advection has 2 implications…

- To the extent that QG theory is valid, we can use the omega equation:

$$(\nabla^2 + f_0/\sigma\, \partial^2/\partial p^2)\omega = f_0/\sigma \partial/\partial p[V_g \nabla(1/f_0 \nabla^2 \Phi + f)] + 1/\sigma \nabla^2[V_g \nabla(-\partial\Phi/\partial p)]$$

The final term says that a local maximum of thickness advection (warm air advection) will tend to be associated with upward motion.

- Also (2), the low-level warm advection acts to destabilize the temperature profile, thereby promoting the release of conditional instability
- Finally, we see that the Initial MCC is on the anticyclonic side of a weak westerly jet stream. Assuming thermal wind balance, this suggests that the MCC develops in a moderate baroclinic zone. Thus, lifting due to baroclinic waves (“short waves”) may provide a mecanism for the release of the conditional instability.

In summary…

- We see that the initial MCC is at a local maximum of low and mid- level moisture, along with a local max in warm advection and a (probable but more speculative) local max in meso-α to synoptic-scale lifting.
- These processes act both to force the release of conditional instabiilty (lifting/destabilization) and to provide a low-mid level moisture source for the maintenance of convection. Again, the important idea is that the convection is focused in a particular region, instead of being random.

Mature MCC

- The strong LLJ (850 mb) continues, along with 700mb warm advection, but the jet max is now on the SW side of the MCC. This differs somewhat from some other studies that found it may still be more on the south side.
- A time-height cross-section for the MCC shows several interesting features:

-- marked decrease in sfc-level θe at the mature stage, due to convective downdrafts

Mature (cont)

-- The mature stage has strong conditional instability in the low-mid levels (i.e., $\partial\theta/\partial z<0$), due primarily to a decrease of the mid-level θe

-- There is a fairly strong inversion near the sfc which acts to decouple the MCC from the sfc. The MCC moisture source is not from the boundary layer but rather from the levels just above the boundary layer (centered around 850mb) → probably due to LLJ

-- At 200 mb, there is a pronounced strengthening of the winds on the NE side of the LLJ, and the creation of a tightly defined jet streak

….The strengthening of the 200mb jet really is quite remarkable from a max speed of ≈ 24 m/s in the initial stage to ≈ 34 m/s at the mature stage.

-- Also at 200mb, there is a noticeable cold core to the MCC. This is probably due to the adiabatic cooling induced by the mesoscale rising motion.

-- On the other hand, there is a warm core at 300 mb. This is due to latent heat and compensating subsidence from small-scale convection. So, what we see is a distinction between organized, mesoscale vertical motions that produce cooling, and the net effect of convective scale elements that produce warming.

- Notice the strong cooling below ≈850mb early in the MCC life cycle. Cotton et al. argue that this represents the evaporative cooling that produces the sfc mesohigh. This is slightly confusing since the cooling is seen only as a relative change from the very warm values at the pre-MCC stage.
- What is the reason for the very warm low-level temps in the pre-MCC stage

- Recall that for a given stage of the MCC life cycle, the composite uses either 00 UTC or 12 UTC sounding data. The perturbations in fig 11 are based on comparison to the MCC-12h stage which is taken from 12 UTC (early morning) soundings. The pre-MCC, initial, and growth stages are from 00 UTC (early eve data). So, the pronounced low-level warming at the pre-MCC stage is due mostly to daytime boundary layer heating.
- Two considerations:

-- for data taken from the same sounding time, the comparisons for the different stages are probably OK

-- after the initial stage, the MCC cloud shield probably suppresses the diurnal cycle sufficiently so that most of the changes are due to the MCC

- The divergence profiles reach their largest absolute values at the mature stage. At the MCC-12h and initial stages, the profiles were dominated by low-level convergence and upper-level divergence in a rather simple, idealized fashion. But, the mature stage shows a more complex structure:

-- low-level (850-1000mb) divergence due to evaporatively driven convective outflows/downdrafts

-- deep mid-tropospheric layer (≈800-400mb) of almost uniform convergence

-- a sharp transition to strong upper-level divergence, maximized near the tropopause (≈200 mb)

- The structure of the divergence profile suggests that the mature stage of the MCC represents a transition from the predominantly convective early stages of the MCC life cycle to a more organized meso-α scale system. The convective elements are driven by boundary-layer convergence, while the moisture supply for the meso-α scale system comes mainly from mid-level inflow (≈600-700 mb)

- The vertical velocity primarily is a reflection of the divergence field. At the initial stage, we see a maximum of upward motion in the low-mid levels (≈600-700mb) which reflects the strong sfc convergence and the upper-level divergence.
- In the mature stage there is strong low-level subsidence due to the high precip rates and evaporative cooling → outflows. The max of upward motion has shifted greatly toward upper-levels (≈300mb)
- So we see a very interesting pattern in the MCC evolution:

-- the MCC is dominated by rising motion throughout most of the troposphere. As the system matures, the level of max rising motion gradually shifts upward. This indicates an evolution of the MCC dynamics from convectively-driven cells to a mesoscale entity with **mid-level inflow**

- The vorticity profile shows a fairly consistent pattern of low-level cyclonic vorticity and upper-level anticyclonic vort. The structure of the vorticity profile is consistent but the magnitude of the upper-level anticyclonic vort. Increases greatly.
- The time-height cross-section of relative vorticity change is more interesting. We see development of strong upper-level anticyclonic vorticity in the mature and dissipating stages. This development of anticyclonic vort apparently is the cause of the pronounced acceleration of the upper-level flow.

MCC Dissipation stage

- In the dissipation stage, the acceleration of the 200mb jet streak persists. The thermodynamic fields show relatively little change from the mature stage
- The divergence field for the dissipating phase is similar to the mature phase, except that the low-level div is no longer present. This points to the relative lack of deep convection in the dissipation stage. The mid-level convergence is reduced slightly but occurs through a somewhat deeper layer, while the upper-level divergence is almost the same as the mature stage

Dissipation (cont)

- Vertical motion reflects the lack of low-level divergence. At dissipation stage, there is upward motion through the entire troposphere region, again. The low-level downdrafts have almost dissappeared. It is interesting to note that the max of upward motion is at almost the identical height and magnitude as the mature stage.
- The vorticity field also shows that the upper-level dynamics are almost unchanged from the mature stage. Notice that the low-level vorticity is reducing toward zero. There seems to be a sense in which the MCC circulation is decaying from the bottom upward.

- Taking this all together, we see that the MCC begins as a primarily convective system with individual cells rooted in or near the PBL. As time goes by, there develops an organized mesoscale circulation with strongest dynamics in the mid-upper troposphere.

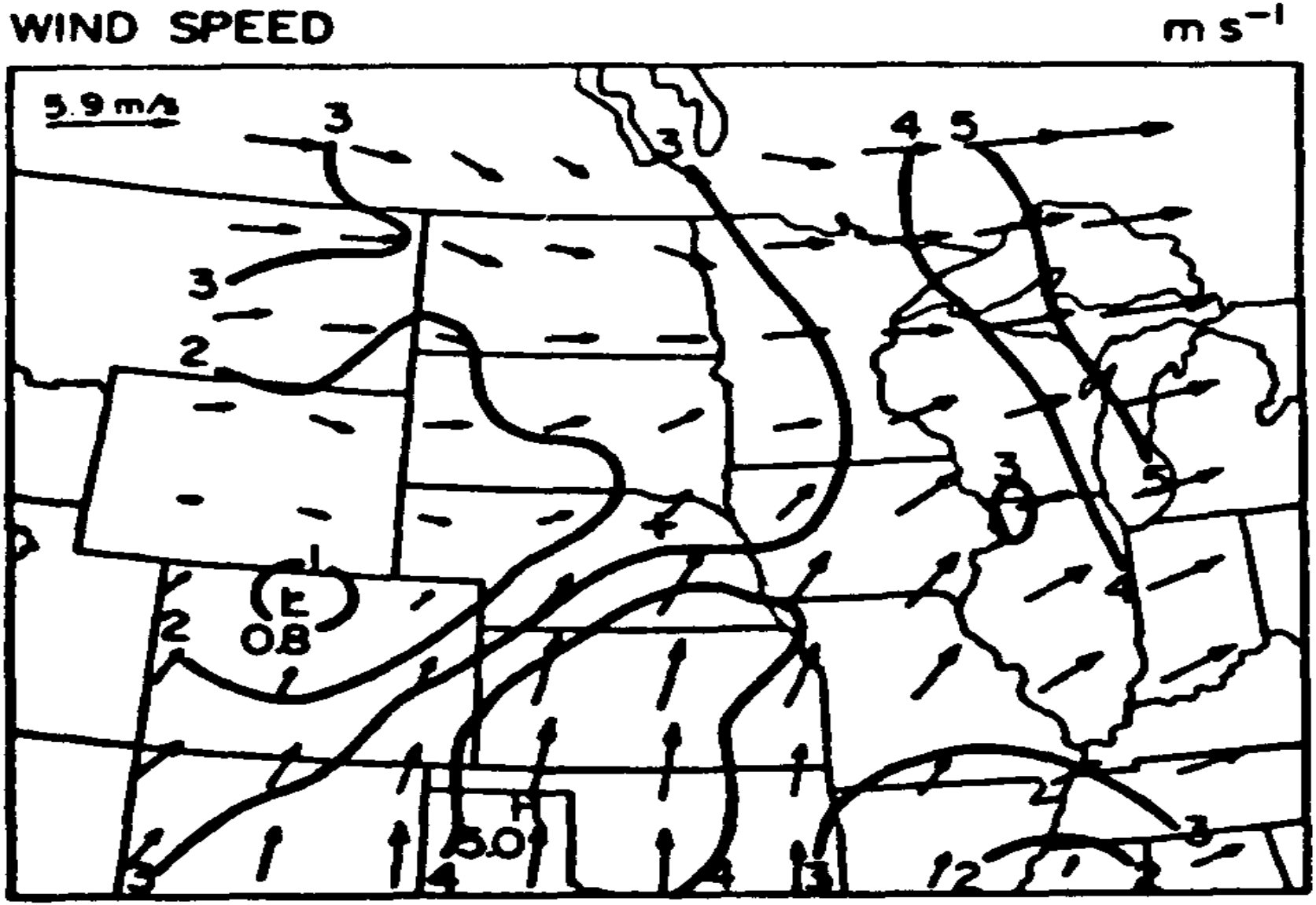

FIG. 3a. Analysis of 850-mb wind speed and wind vectors at the initial stage. The center grid point (+) marks the average position of the MCC centroid at the initial stage. Units: m s^{-1}.

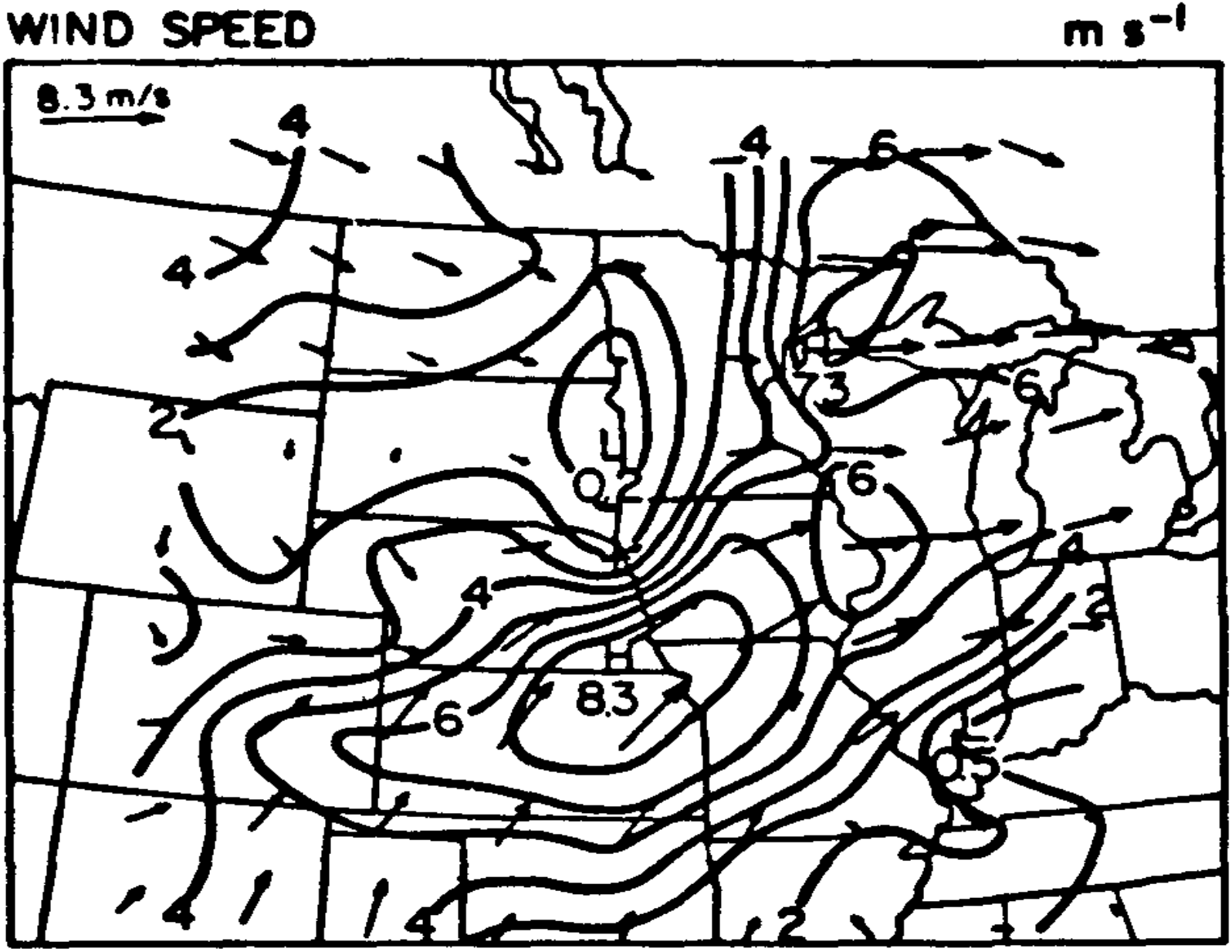

FIG. 3b. As in Fig. 3a, except for the growth stage. Units: m s^{-1}.

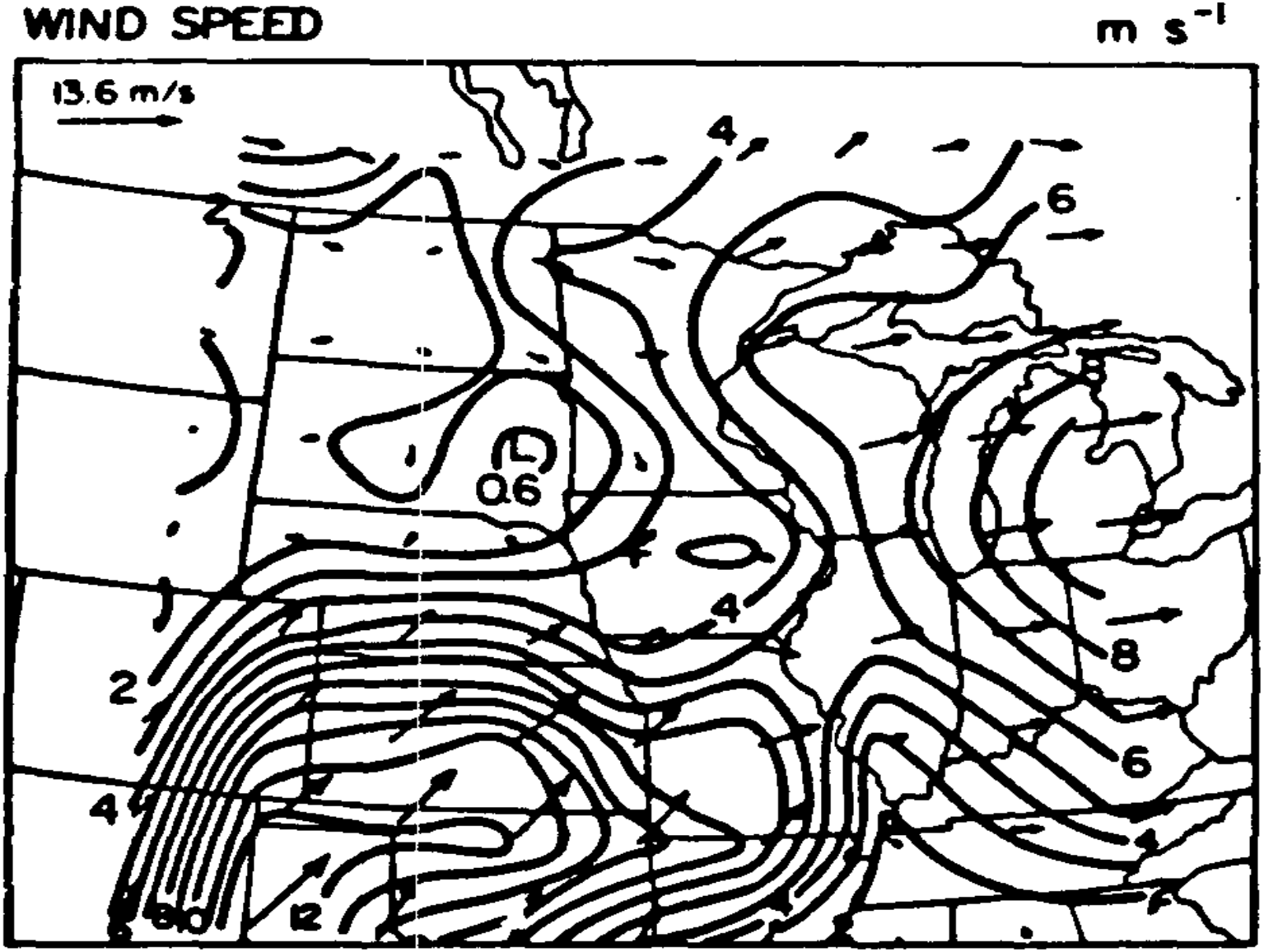

FIG. 3c. As in Fig. 3a, except for the mature stage. Units: m s^{-1}.

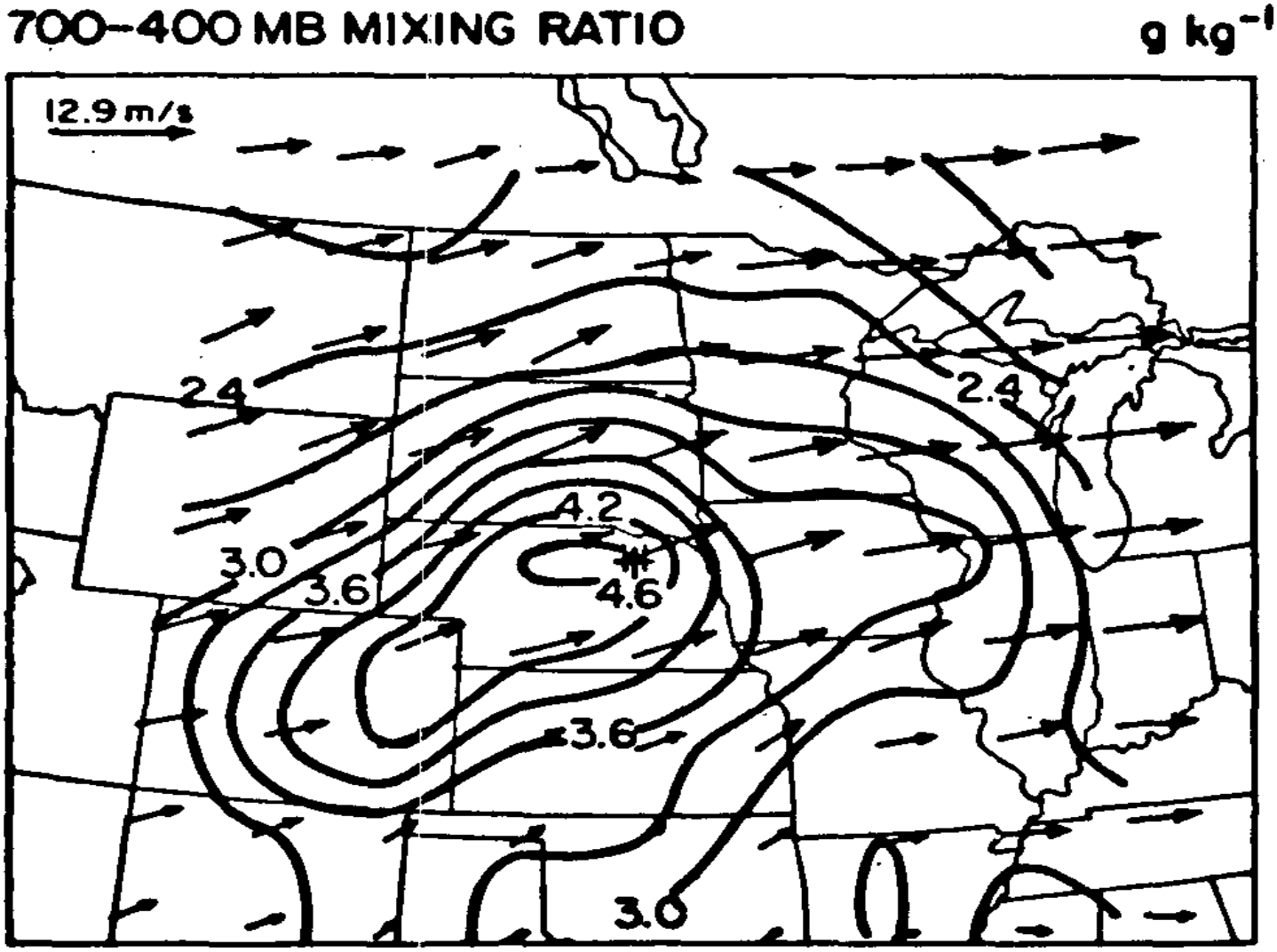

FIG. 4. Analysis of the average 700–400 mb mixing ratio and wind vectors at the initial stage. The layer-mean mixing ratio and wind vectors are calculated by averaging q, u and v at 50-mb increments through the layer. The center grid point (+) marks the average position of the MCC centroid at the initial stage. Units: g kg^{-1} and m s^{-1}.

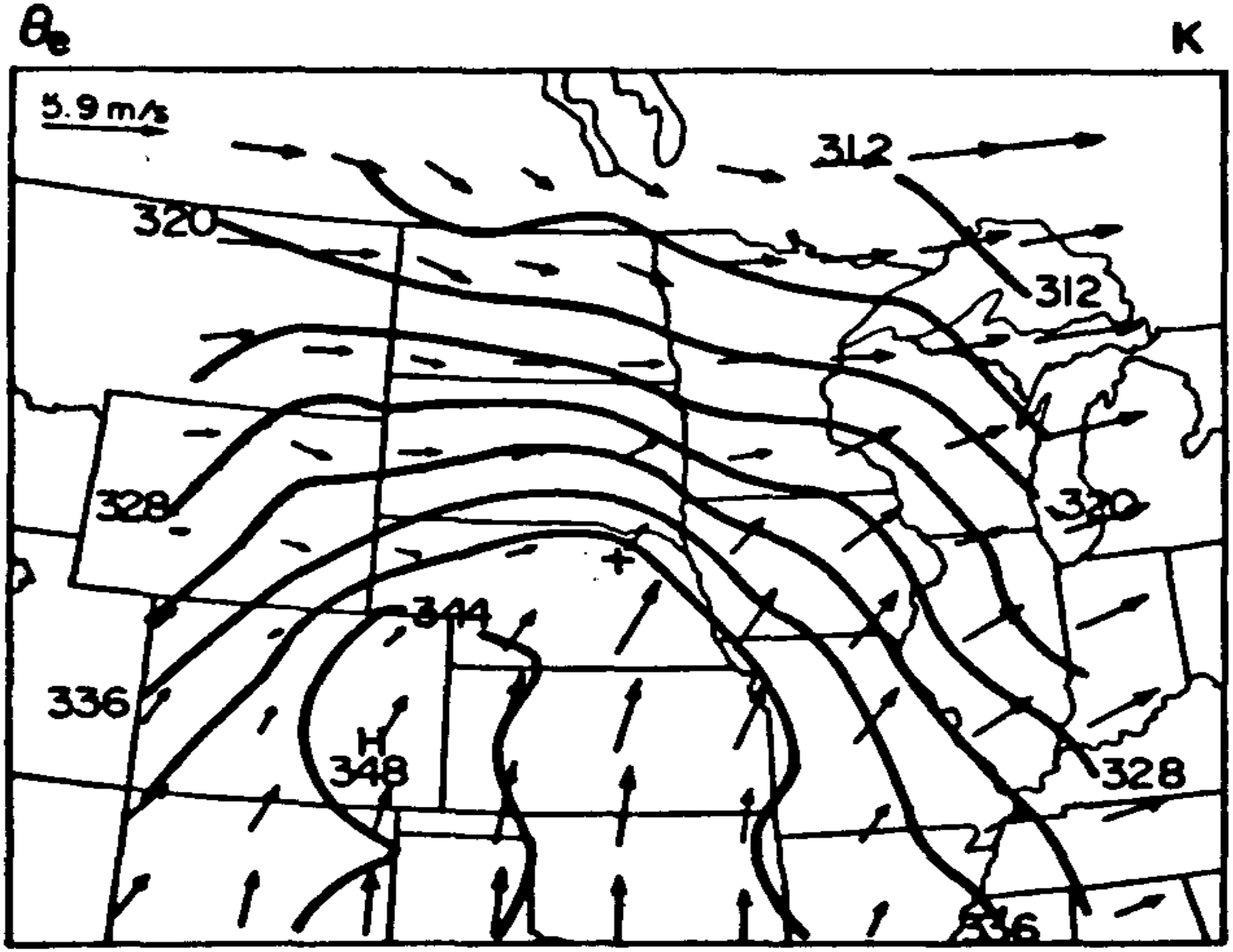

FIG. 6. Analysis of 850-mb equivalent potential temperature (θ_e) and wind vectors at the initial stage. Units: K and m s^{-1}.

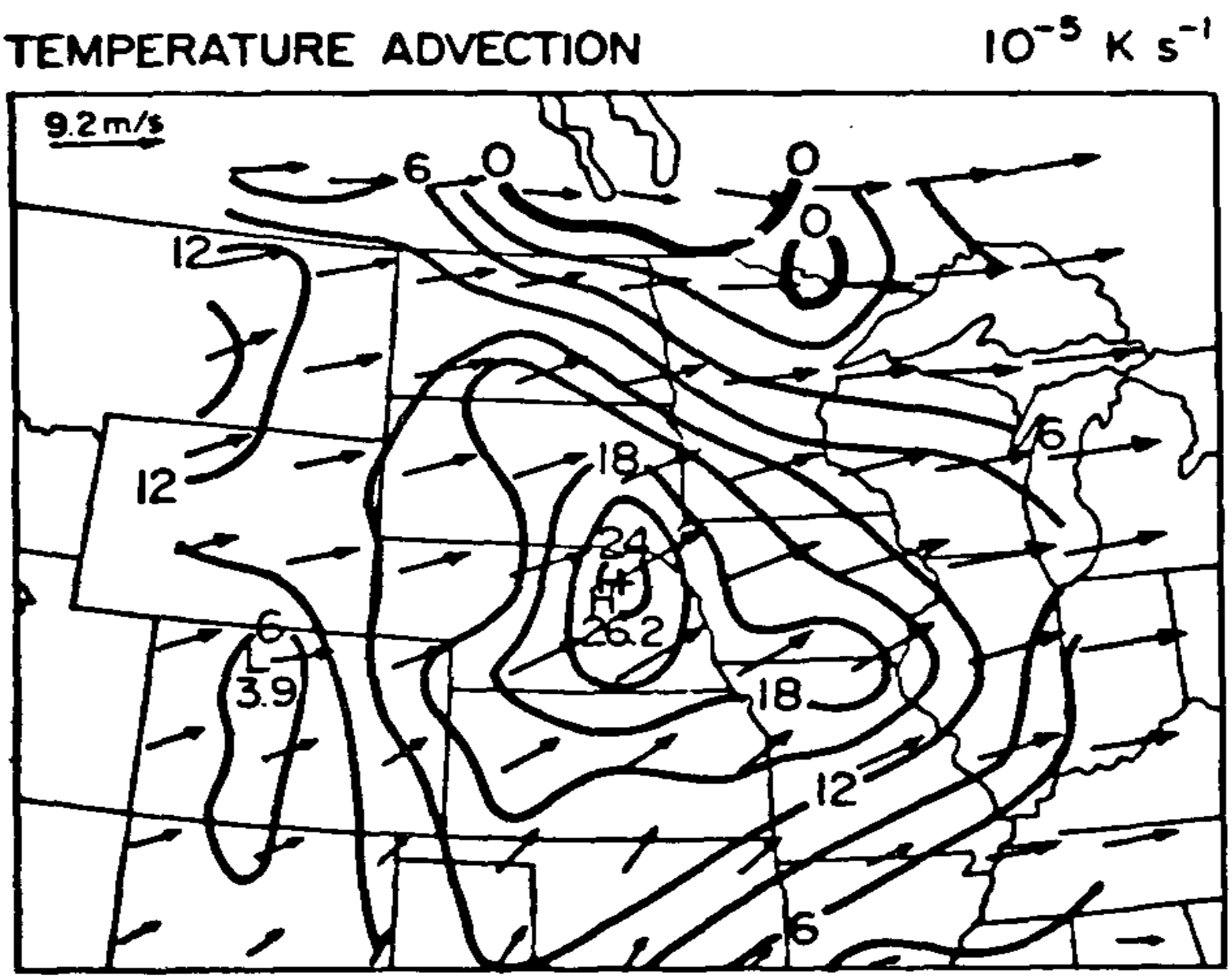

FIG. 7a. Analysis of 700-mb temperature advection and wind vectors at the initial stage. Units: 10^{-5} K s^{-1} and m s^{-1}.

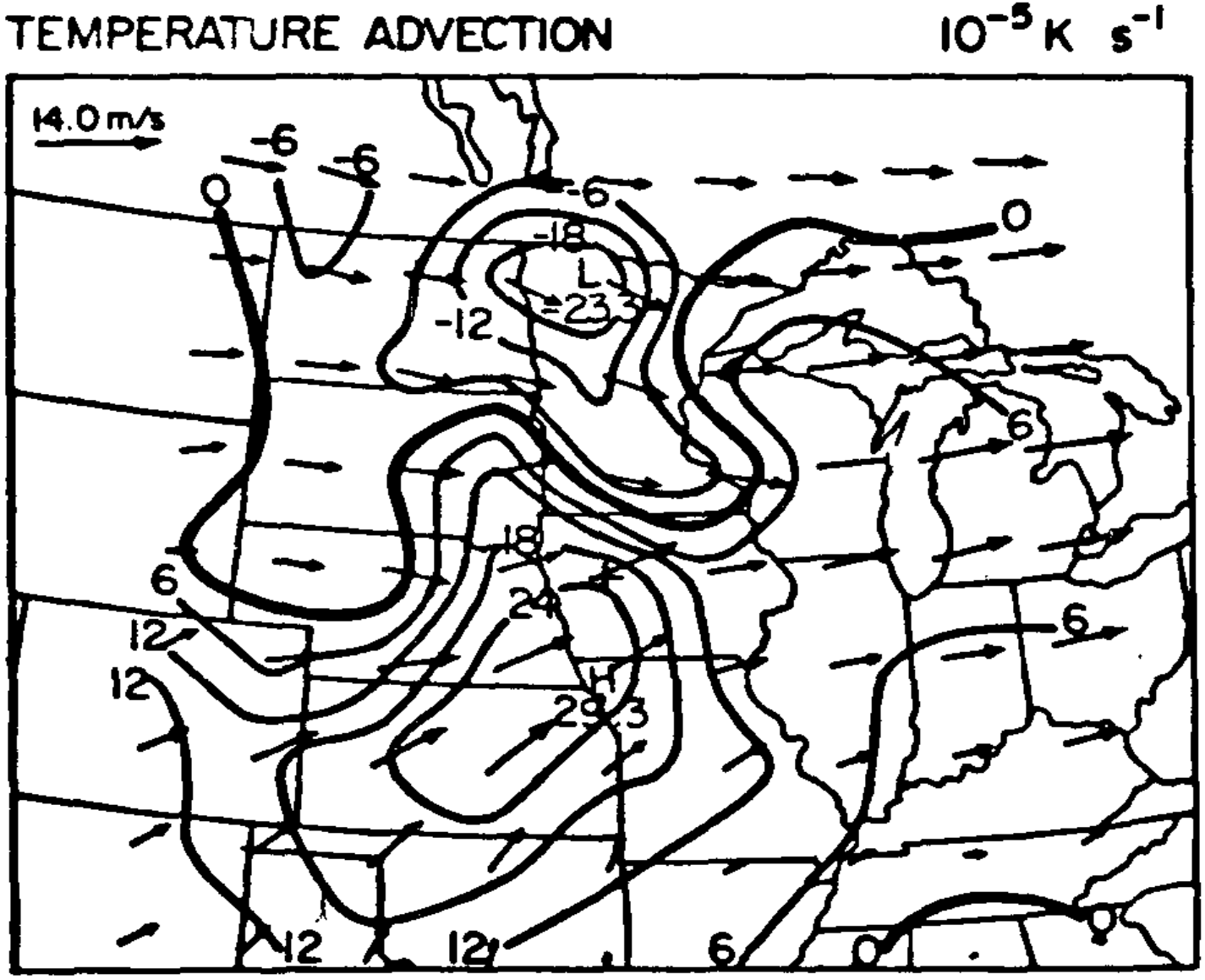

FIG. 7b. As in Fig. 7a, except for the mature stage. Units: 10^{-5} K s^{-1} and m s^{-1}.

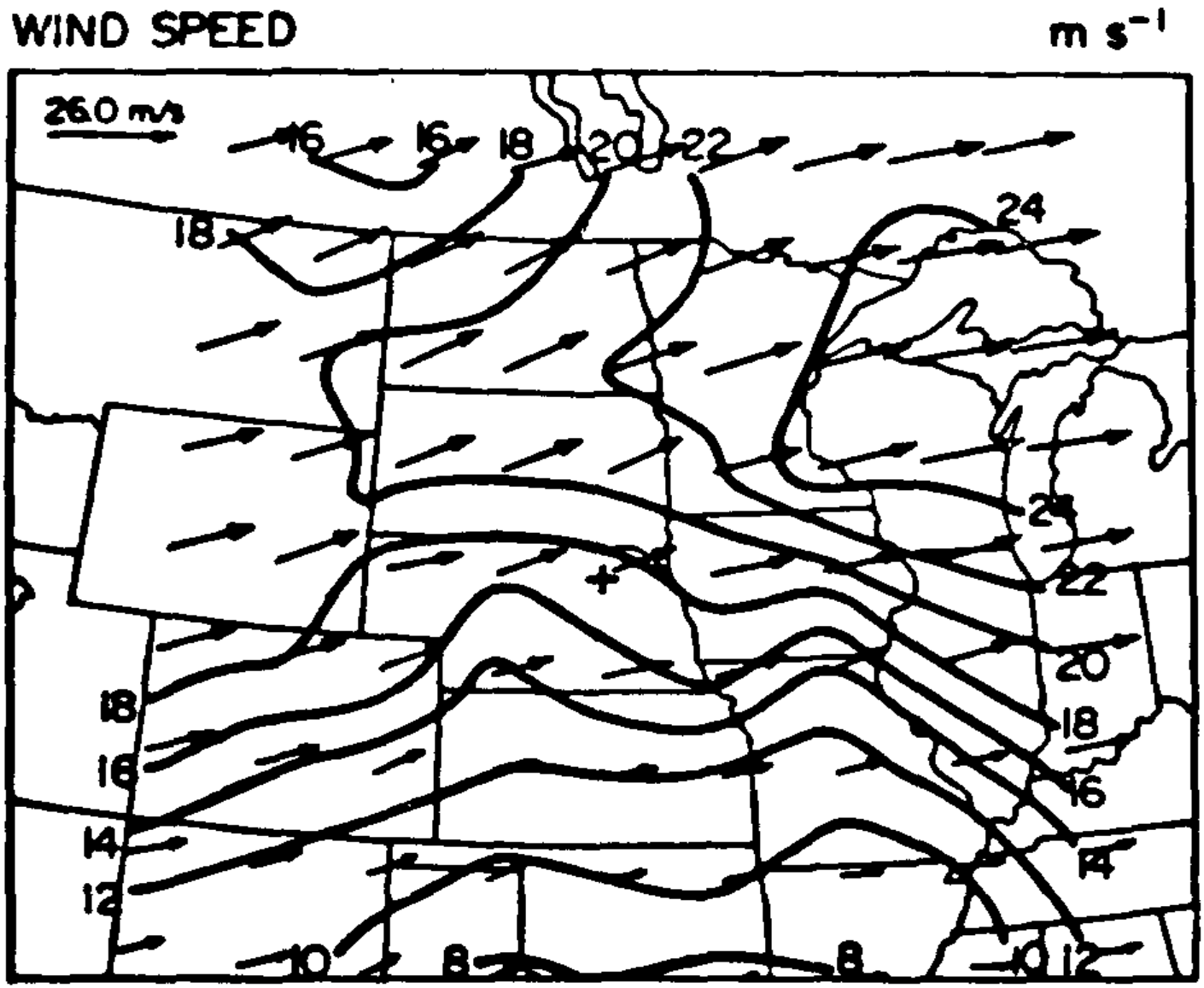

FIG. 9a. Analysis of 200-mb wind speed and wind vectors at the initial stage. Units: m s^{-1}.

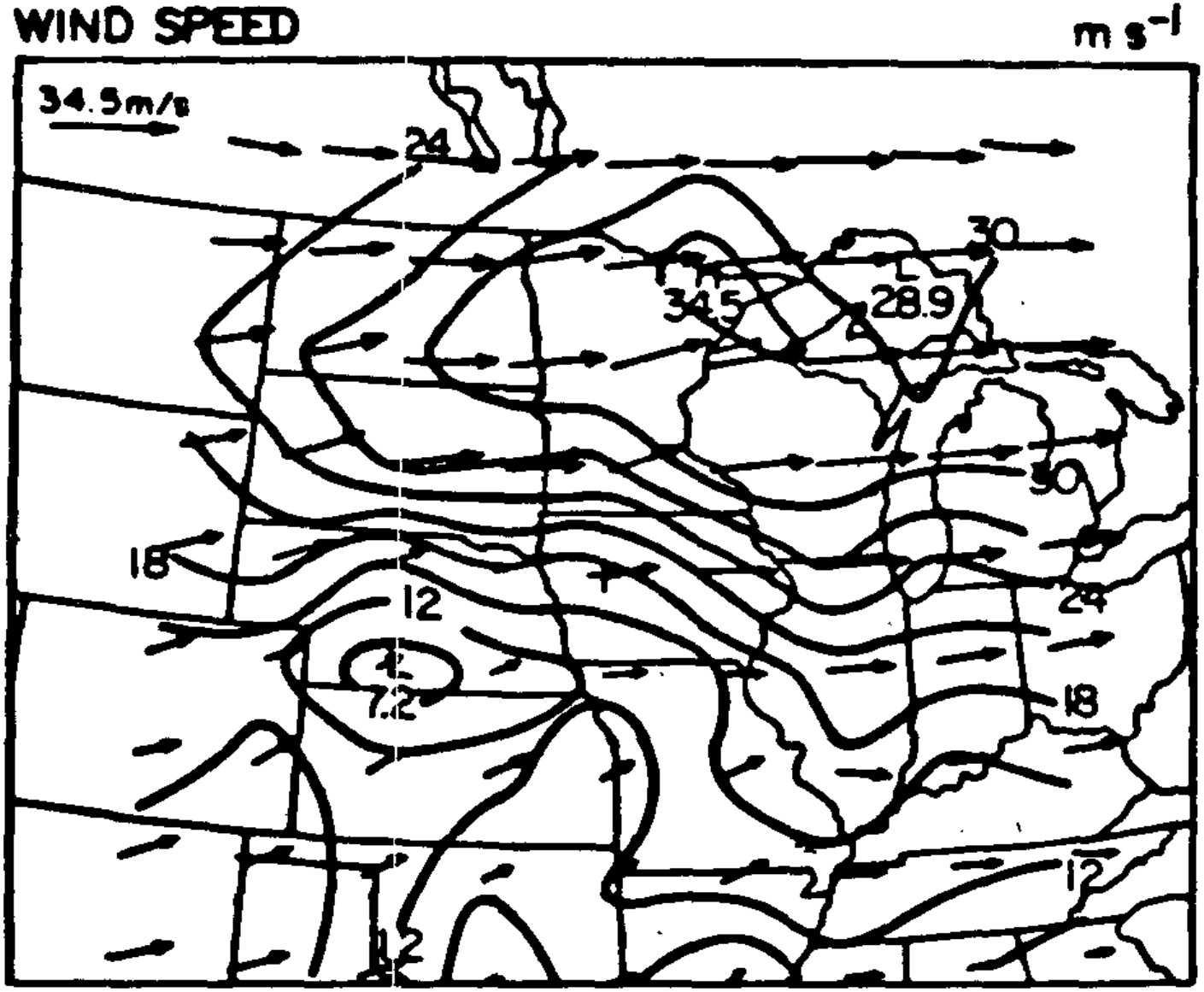

FIG. 9b. As in Fig. 9a, except for the mature stage. Units: m s^{-1}.

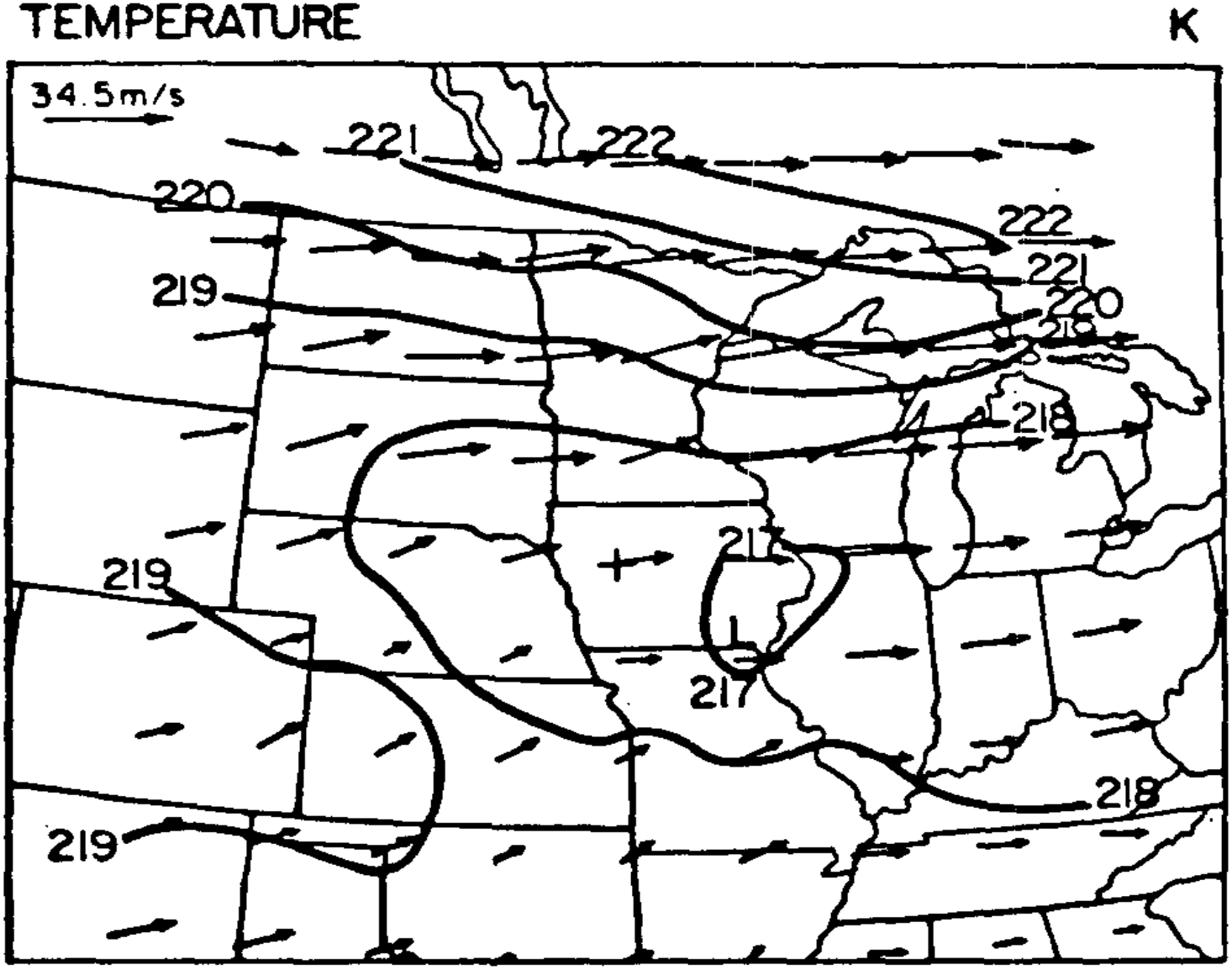

FIG. 10a. Analysis of 200-mb temperature and wind vectors at the mature stage. Units: K and m s^{-1}.

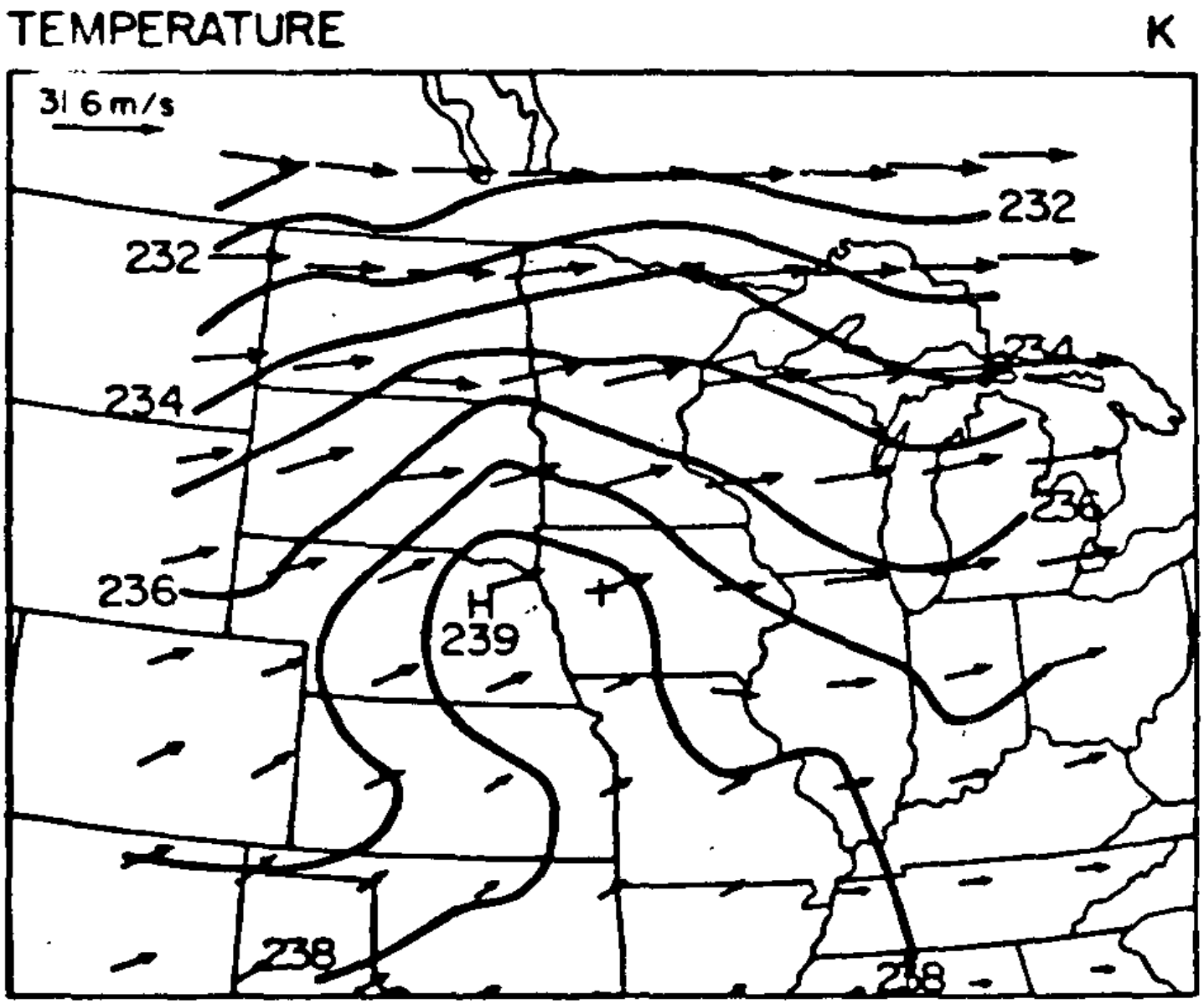

FIG. 10b. As in Fig. 10a, except for the 300-mb level. Units: K and m s^{-1}.

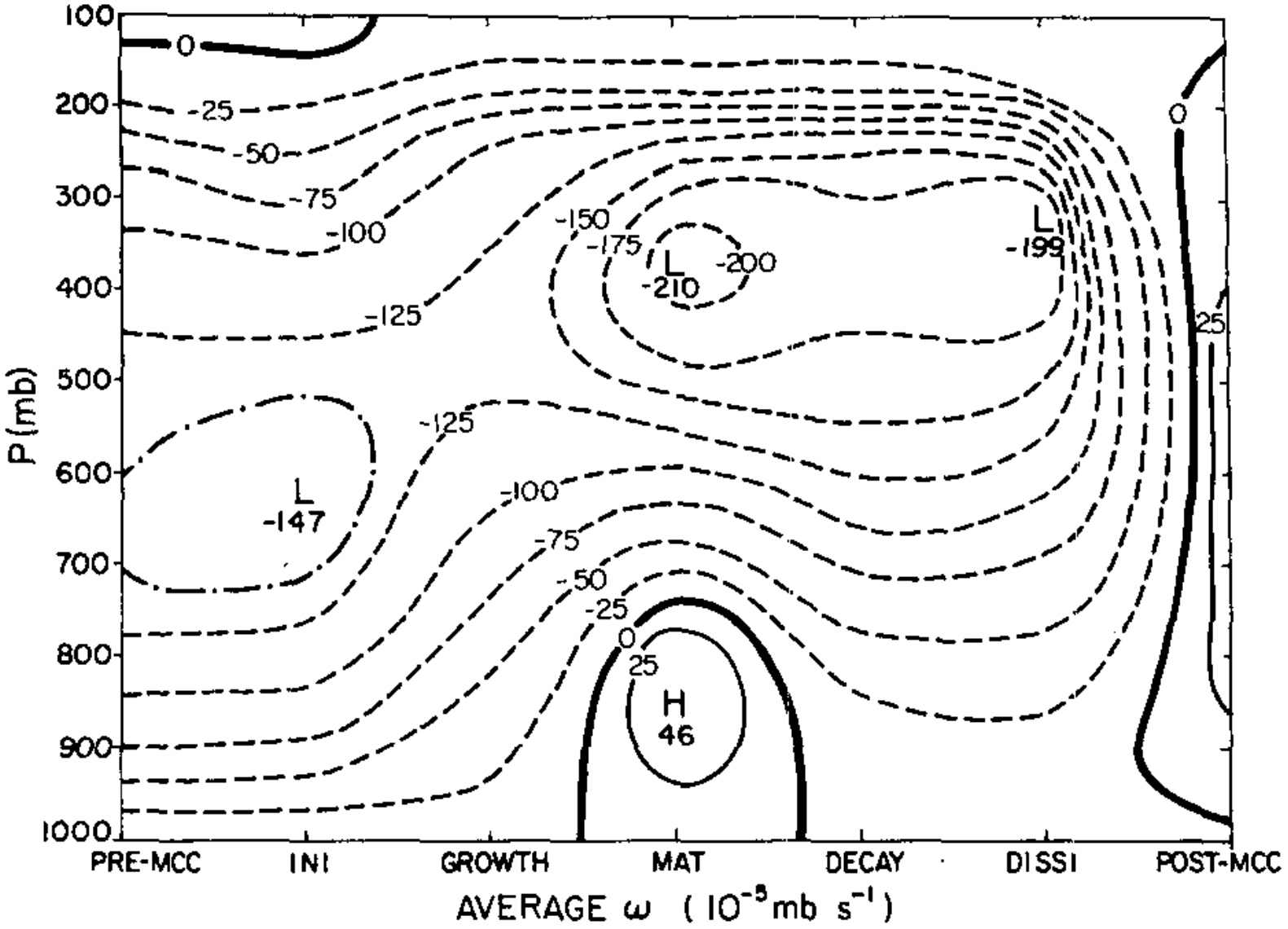

FIG. 14. Time–height plot of vertical motion. Each subperiod ω profile was obtained as in Fig. 13. Units: 10^{-5} mb s^{-1}.

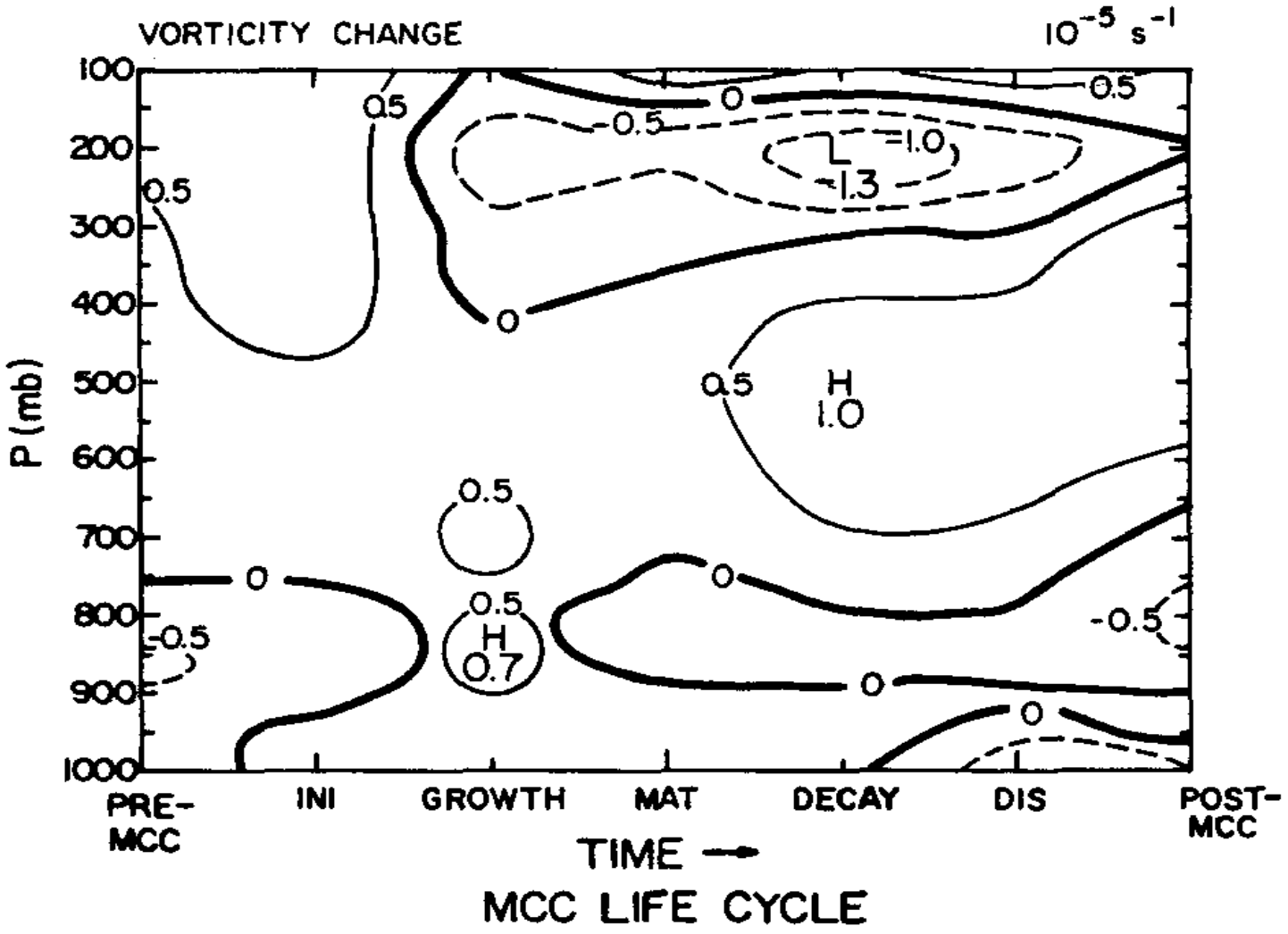

FIG. 16. Time–height plot of the difference in relative vorticity (horizontally averaged over the 3 × 3 central grid points at each 50-mb level and subperiod) from its corresponding value at the MCC-12 h stage. Positive values indicate a more cyclonic (or less anticyclonic) vorticity than at the MCC-12 h stage. Units 10^{-5} s^{-1}.

MCC moisture budget:

Cotton et al. adopted a conservation equation for water vapor as:

$$\overline{P} - \overline{E} = -\int_{P_{sfc}}^{P_{100}} q(\nabla \cdot \vec{V}) \frac{dp}{g} - \int_{P_{sfc}}^{P_{100}} \vec{V} \cdot \nabla q \frac{dp}{g} - \frac{\partial}{\partial t}\left[\int_{P_{sfc}}^{P_{100}} q \frac{\partial p}{g}\right]$$

(1) mass-flux conv. (2) advection (3) storage

What are the units of the RHS terms?

$$\text{e.g., } q(\nabla \cdot \vec{V}) \frac{dp}{g} \approx q(\nabla \cdot \vec{V}) \frac{\rho g \, dz}{g} = \rho q (\nabla \cdot \vec{V}) \, dz$$

$$= (kg\ m^{-3})(s^{-1})(m)$$

$$= kg\ m^{-2}\ s^{-1}$$

So the units of P, E must be $kg\ m^{-2}\ s^{-1}$ (rainfall rate is multiplied by the density of water).

In this analysis the evaporation term is the residual after subtracting the RHS term from the precip rate, and thus includes the accumulated measurement errors as well as the real evaporation.

Throughout the MCC life cycle, the convergence term (1) is the primary source for water vapor. Advection is a large source term in the early stages and then diminishes to become a sink or near-zero in the mature to dissipation stages. The storage term is very large and positive (recall it appears as $-\frac{\partial q}{\partial t}$ in the budget) for the pre-MCC phase and gradually decreases to become small or negative from the mature phase onward. The precip rate shows a sharp peak right at the mature phase and is remarkably symmetrical about the time of the mature phase.

The storage term relates in a number of ways to the interaction of the convective system with its environment. We can think of the MCC as defining a "control volume" for which we can account for the moisture

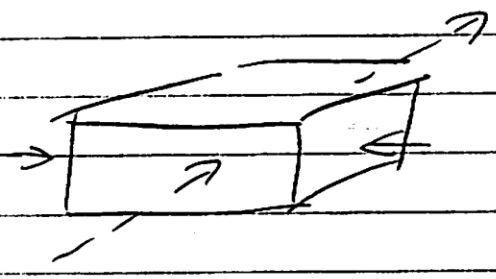

Any water vapor that is supplied by convergence of mass into the volume, or by advection, must be either (1) stored in the volume, or (2) removed as precip. (Notice that there is an additional source of water vapor due to evaporation of liquid water in the volume. More on this later.)

Therefore we can partition the moisture supply into
(1) the fraction of the moisture supply that goes into moistening the volume (⇒ storage), and
(2) the fraction that falls as precip.
This partitioning is the basis for the well-known Kuo scheme of cumulus parameterization. The "b" parameter is the fraction of the moisture supply that goes into moistening the environment. Then (1 - b) is the precip efficiency of the system, i.e. the fraction of the moisture that gets rained out. Quantitatively,

$$\frac{dq}{dt} \approx -(C-E) - \frac{\partial F_q}{\partial p} \qquad (F_q \equiv \text{turbulent fluxes})$$

This is following a parcel. For a column,

$$-\int_0^{p_s} (C-E)\, dp = (1-b)\left[\int_0^{p_s} \nabla_2 \cdot (\vec{V}_2 q)\, dp + F_{q_s}\right]$$

Note that $\int F_q\, dp = F_{q's}$ - since the only source / sink is at the boundary (surface).
The term in brackets is the total water vapor input to (or extraction from) the column.
The quantity

$$M_t = \frac{-1}{g}\left[\int_0^{p_s} \nabla \cdot (\vec{V} q)\, dp + F_{q_s}\right] \qquad \frac{1}{m}\ m\ s^{-1}\ kg\ m^{-1}\ s^{-2} \Rightarrow \boxed{kg\ m^{-2}\ s^{-1}}$$

is called the moisture accession in the Kuo scheme.

(What are the units of M_t ? ⇒ interpretation)

Then we have

$$\boxed{-\int_0^{P_s} (C-E)\, dp = -(1-b)\, g\, M_t}$$

Then the net production of condensate in the column is the total moisture input M_t multiplied by the factor $(1-b)$.

So $(1-b)$ is essentially the precip efficiency. But we saw earlier that the precip efficiency varies dramatically during the MCC life cycle.

Anthes (1977) modified the Kuo scheme to make "b" a function of the relative humidity:

$$b = \begin{cases} \left[\dfrac{1-\langle RH\rangle}{1-RH_c}\right]^n & \langle RH\rangle \geq RH_c \\ 1 & \langle RH\rangle < RH_c \end{cases}$$

where $\langle RH\rangle$ is the vertically-averaged relative humidity and RH_c is a "critical" relative humidity.

For the MCC we find that the precip efficiency is about 5% in the early stages and increases steadily to 113% in the mature stage.

How can we get precip efficiency > 100%?

The precip efficiency is defined as

$$PE = 1 - \frac{\text{storage}}{\text{water vapor supply}}$$

where the "supply" is the sum of convergence, advection and evaporation (again, evap is a source of water vapor). Then PE > 1 only if the storage term is negative. This implies that the "b" parameter in the Kuo scheme would be negative (i.e., $(1-b) > 1$).

It would have been interesting to see how the PE varied with the $\langle RH \rangle$ so we could evaluate whether Anthes assumption was realistic.

TABLE 4. The water vapor budget and its comparison with observed precipitation during MCC evolution. Units in depth (mm) of liquid water per 3 h.

Subperiod	Term (1) $-q\nabla\cdot\mathbf{V}$	Term (2) $-\mathbf{V}\cdot\nabla q$	Term (3) $-\partial q/\partial t$	Terms (1 + 2 + 3) P-E	Observed P	Calculated E
Pre-MCC	1.505	1.227	−3.078	−0.346	0.580	0.926
Initial	1.238	0.464	−1.060	0.641	1.549	0.908
Growth	2.125	0.176	−0.712	1.589	2.614	1.025
Mature	1.620	−0.781	0.348	1.187	3.017	1.830
Decay	1.824	−0.357	−0.403	1.065	2.575	1.510
Dissipation	1.192	0.027	−0.716	0.503	1.545	1.042
Post-MCC	−0.119	0.268	−1.028	−0.879	0.967	1.846

Converge. advect storage precip evap

TABLE 5. The water vapor budget during MCC Evolution. Units in %.

Subperiod	conv Term (1) (%)	adv Term (2) (%)	1 + 2 Term (1 + 2) (%)	storage 3 Term (3) (%)	E	PE
Pre-MCC	41.1	33.6	74.7	−84.1	25.3	15.9
Initial	47.4	17.8	65.2	−40.6	34.8	59.4
Growth	63.9	5.3	69.2	−21.4	30.8	78.6
Mature	60.7	−29.3	31.4	13.0	68.6	113.0
Decay	61.3	−12.0	49.3	−13.5	50.7	86.5
Dissipation	52.7	1.2	53.9	−31.7	46.1	68.3
Post-MCC	−6.0	11.9	5.9	−51.5	94.1	48.5

MCC Precipitation

- McAnelly and Cotton looked at precip patterns for 122 MCC events. Their sample was restricted to:

-- summertime (Jun-Aug). Springtime MCCs tend to occur in more strongly baroclinic environments. Thus, they focused on MCCs that were of more "pure" convective forcing, rather than significant large-scale (presumably baroclinic) forcing. Notably, an earlier study (Kane, Chelius, and Fritsch 1987) found that the springtime MCCs with stronger synoptic forcing were rainier than the summertime MCCs.

-- cases which fit an idealized MCC life cycle similar to that of Cotton et al. (1989). This was done so that they could evaluate the changing character of the precipitation through the MCC life cycle. They rejected MCCs that redeveloped or that merged with other MCSs.

- All in all, they kept about ¾ of the Jun-Aug MCCs in the annual summaries. Each MCC life cycle was divided into 14 subperiods:

*1-3 h before (each period 1 ½ hours)

*Start (“initial” in Cotton et al.)

*4-7 h between

* Max IR cloud shield (“mature” in Cotton)

* 8-11 h after

* end

- M&C also defined a mesoconvective stage which essentially corresponded to the most strongly developed portion of the MCC. The definition of this mesoconvective stage was somewhat subjective:

  - a relatively smooth and circular shape to the -52C cloud shield

  -- a relatively strong and uniform thermal gradient in the outer part of the IR cloud shield

This stage usually is from the middle of the MCC growth phase until just after the time of the max -52C cloud shield (sometimes before, sometimes after). It is interesting to note that the end of the mesoconvective stage corresponds with the transition in MCC dynamics/thermodynamics that was found at the mature stage (max cloud shield) in the composite analysis of Cotton et al.

- They also defined the “thermal minimum” as the time when the cloud top was coldest and largest. Again, this was subjective, e.g., not just one very cold pixel but some evidence of a mesoscale feature with cold temps over a “widespread area”. The thermal minimum reflects the time of the most intense and organized deep convection. On average, this occurred just before the max -52C cloud shield

- The data source for the study was based on hourly precip data from gages with 0.25mm (0.01 in) or 2.5 mm (.1 in) resolution. The rainfall data were analyzed in two ways:

* Bulk precip analysis – done over 3 circular domains centered on the MCC position at a particular hour. Size of the domains varied with the size of the -33 C (not -52C) cloud shield, but shape was always circular regardless of the shape of each MCC. This analysis yields one value for the rainfall in the circle

* Mapped precip analysis – done with a moving 10x10 grid centered on the storm, each grid cell is $(0.625^{o}\ \text{lat})^{2}$. This allows the spatial variability of the precip to be evaluated.

- M&C found that in general, the highest precip intensity (mm/hr) occurred in the growth stage of the MCC, while the greatest areal extent of the precip and total volumetric rain rate for the storm were maximized around or shortly after the max -52 C cloud shield. Most of the precip was attributable to the innermost of the 3 circular domains.
- Notice that the volumetric rate undergoes a transition during the MCC life cycle. In the earlier stages, the innermost domain is clearly dominant. But after the maximum extent (and especially after the mesoconvective stage), the outer domains contribute as much or more than the inner domains

- The maximum of the rainfall rate in the first half of the MCC life cycle is due not to a uniform rise or fall of precip rates, but rather to a greater number of measurements with high rates. M&C use the 7.6mm/h (0.3in/h) rate as a practical discriminator between convective and stratiform precip.
- The convective-mesoscale transition is reflected in the areas that exceed given thresholds. The higher thresholds are maximized somewhat before the max cloud shield and the lower thresholds are maximized around or somewhat after the max cloud shield.
- The areal distribution of “convective” and “stratiform” precip (so-called) shows some very interesting patterns. In the early stages, both the convective and stratiform precip are maximized to the south of the MCC centroid. This makes sense, because the south is the “inflow” side, from the perspective of the LLJ

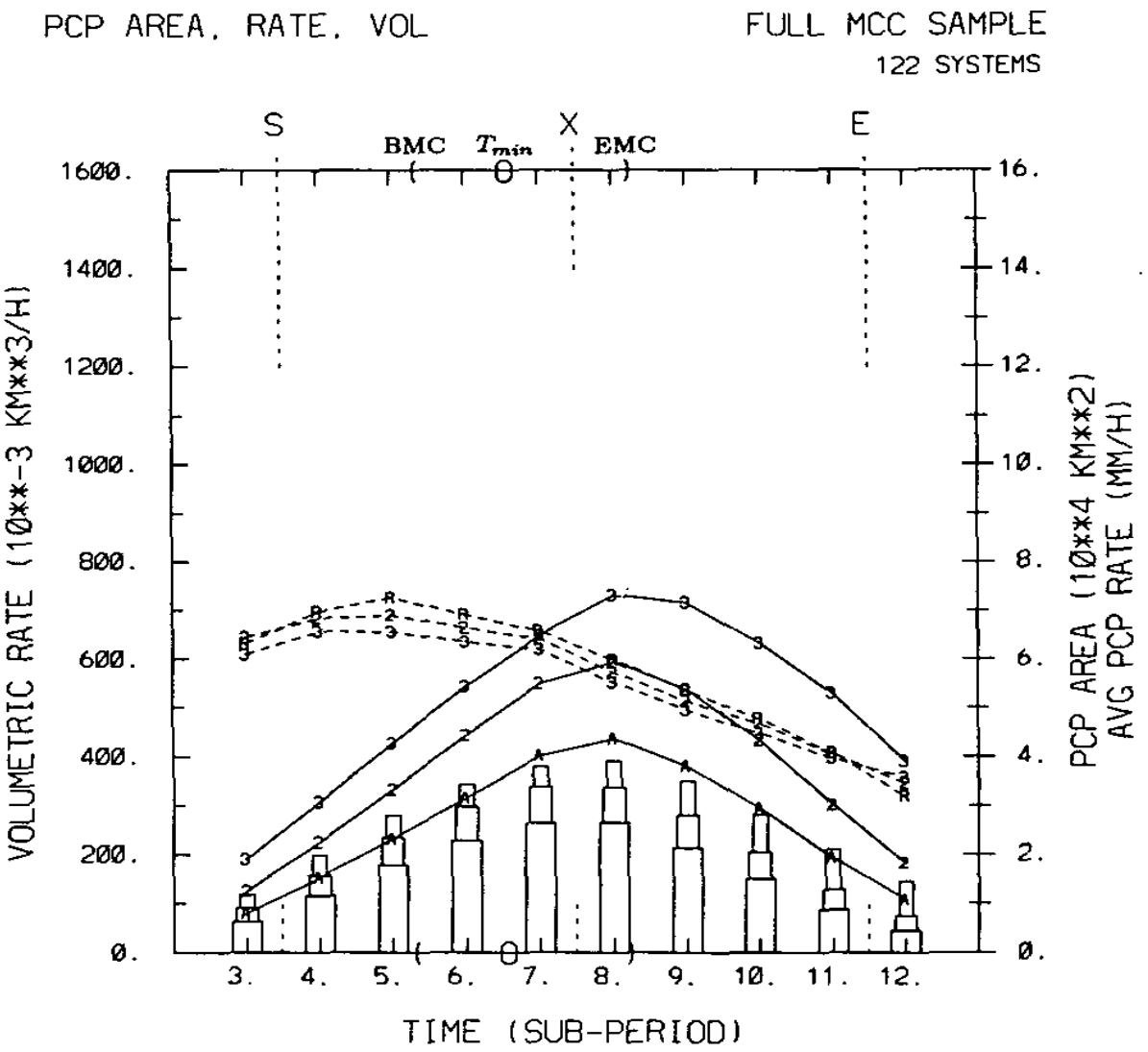

FIG. 9. Bulk precipitation characteristics for 122-case composite MCC over all three domains, for combined-gage sample. Display is similar to Fig. 8. Primary curves are for smallest domain. Analysis for the midsize and largest domains are shown by the additional curves (labeled 2 and 3, and second and third departure bars, respectively).